



## Vulnerability Index Assessment for Mapping Ground Movements Using the Microtremor Method as Geological Hazard Mitigation

Adi Susilo<sup>1\*</sup>, Siti Zulaikah<sup>2</sup>, A. Fauzi Pohan<sup>3</sup>, M. Fathur Rouf Hasan<sup>1, 4</sup>,  
Farizky Hisyam<sup>1</sup>, Siti Rohmah<sup>1</sup>, M. Aryono Adhi<sup>5</sup>

<sup>1</sup> Department of Physics, Faculty of Mathematics and Natural Sciences, Universitas Brawijaya, Malang, 65145, Indonesia.

<sup>2</sup> Department of Physics, Faculty of Mathematics and Natural Sciences, Universitas Negeri Malang, Malang, 65145, Indonesia.

<sup>3</sup> Department of Physics, Faculty of Mathematical and Science, Andalas University, Padang, 25163, Indonesia.

<sup>4</sup> Department of Civil Engineering, Politeknik Negeri Jakarta, Depok, 16425, Indonesia.

<sup>5</sup> Department of Physics, Faculty of Mathematics and Natural Sciences, Semarang State University, Semarang, 50229, Indonesia.

Received 21 January 2024; Revised 21 April 2024; Accepted 26 April 2024; Published 01 May 2024

### Abstract

Various geological disasters, such as landslides and ground movements, occur annually in Srimulyo Village, Malang District, with varying levels of damage. Ground movements can affect structures built above, causing sinking, cracking, and collapse. Research into landslides and ground movements triggered by vibrations is generally conducted using the microtremor method, which has proven effective. This study uses the microtremor method to map the soil condition that is potentially prone to movement or landslides based on the observed soil vulnerability index. Data was collected using a TDL 303s Digital Portable Seismograph instrument; the measurement points were established in the form of a grid distributed across the research area, with a recording duration of approximately 45 minutes at each point. The analysis technique utilizes the Horizontal Vertical Spectrum Ratio (HVSr) based on the Fast Fourier Transform (FFT) principle. The study's results found that the research location's seismic vulnerability index varies between 6.5 and 16.5. Areas with high seismic vulnerability index values, specifically those with  $K_g > 11.5$ , are scattered on the west, south, and southeast sides of the research location. Based on field observations, these areas are dominated by relatively thick sediment layers, leading to lower dominant frequency values and higher amplification values; consequently, the seismic vulnerability index in the southern region is also high.

**Keywords:** Geological Hazard Mitigation; Ground Movements; Microtremor; Vulnerability Index.

## 1. Introduction

The geological conditions of Malang District are characterized by its proximity to active volcanoes such as Mount Semeru, Mount Bromo, Mount Arjuno, and Mount Welirang, all of which can erupt at any time. Additionally, Malang District is surrounded by several active faults. This situation further solidifies the district's position as one of the areas most prone to geological disasters. According to data from the Regional Disaster Management Agency (BPBD), Malang Regency experiences approximately 100 geological disasters annually, including landslides, earthquakes, subsidence, and volcanic eruptions, with estimated annual losses reaching around 3 million USD [1]. Geological disasters such as earthquakes and landslides not only result in financial losses but also lead to loss of life [2, 3]. Various geological

\* Corresponding author: [adisusilo@ub.ac.id](mailto:adisusilo@ub.ac.id)

<https://dx.doi.org/10.28991/CEJ-2024-010-05-017>



© 2024 by the authors. Licensee C.E.J, Tehran, Iran. This article is an open access article distributed under the terms and conditions of the Creative Commons Attribution (CC-BY) license (<http://creativecommons.org/licenses/by/4.0/>).

disasters are almost imminent in every village in Malang Regency, East Java, Indonesia, one of which is Srimulyo Village, Dampit District [4]. This village experiences landslides or soil movements almost every year, with varying losses. This situation requires further subsurface investigations to plan disaster mitigation and preparedness. When the soil structure undergoes movement, it has implications for the buildings, such as sinking, cracking, and collapsing. Earthquakes or active fault lines typically influence soil movement. Recently, soil movement has also occurred due to slope inclination and surface soil load, resulting in soil instability. The phenomenon of soil movement has the same impact as landslides, causing permanent surface soil damage and becoming increasingly severe if it occurs within residential areas. This condition will continue if there is no disaster mitigation at its source. Geological disasters cannot be entirely prevented, but some measures can be taken to reduce their impact [5], such as investigating the condition of subsurface soil layers in detail to estimate the root causes.

The microtremor method is commonly used to investigate and evaluate landslides [6] and soil movement triggered by earthquakes, and it has proven to be effective. The microtremor method provides data in the form of signals for three components (North-South, East-West, and Up-Down) in the time domain. Based on these three signal components, dominant frequency ( $F_0$ ) and amplification factor ( $A_0$ ), values are obtained, and both values are used to calculate the seismic vulnerability index ( $K_g$ ) used to identify soil that is vulnerable to movement. Microtremors, known as ambient noise or vibrations originating from within the ground with specific amplitudes, have been useful in determining soil layers' fundamental frequency and amplitude [7]. Liu et al. (2023) used the microtremor method to measure the soil vulnerability index on a potential landslide road section. The research indicates that the vulnerability index is related to road damage and soil movement behavior. The soil vulnerability index is a warning parameter to identify potential landslide locations [8]. In addition to landslide hazards, microtremor surveys can also be used for seismic hazard assessments. This is particularly useful in basin regions with both surface and hidden faults. For instance, Pornsopin et al. (2024) conducted a microtremor analysis in Thailand's Chiang Mai Basin area to create a seismic microzonation map. The results provided insights into the basin's structure and thickness of soil layers [9]. In previous research, the author used the microtremor method to detect damage triggers in Wirotaman Village, Malang Regency, due to an earthquake with a magnitude of 6.1 Mw. In this research, the author found that local faults influenced ground surface movements, thereby triggering greater damage to the line crossed by the local faults due to that earthquake [10].

Several studies on the seismic vulnerability index indicate a correlation between the values of the index and the level of building damage in an area. Livaoğlu et al. (2019) and Güven (2022) demonstrated a positive correlation between the seismic vulnerability index in northwest Turkey and the severity of structural damage caused by the 1999 Kocaeli earthquake [11, 12]. The seismic vulnerability index also correlates with soil thickness in a region. Arisalwadi & Sastrawan (2023) applied information on soil thickness and geological conditions based on the seismic vulnerability index data to create a seismic microzonation map for Indonesia's new capital region in North Penajam Paser [13]. The seismic vulnerability index can provide information about local effects that influence seismic vulnerability in a region. Siburian et al. (2024) linked the distribution of seismic vulnerability index values to the ground shear strain (GSS) values of historical earthquakes in the Suban area, Curup Rejang Lebong, Bengkulu, Indonesia. These studies show that besides building construction, soil's physical and mechanical properties also play a crucial role in influencing the level of building damage due to geological disasters, especially earthquakes [14].

Theoretically, solid rock structures are good mediums for seismic wave propagation. Generally, earthquake shaking is more strongly felt in such areas, making buildings on them more susceptible to damage. This situation is different when the layers above compact rock is made up of clay, sand, or deposits. The interface between these two rock types can create a sliding plane. This condition is more hazardous because the surface appears safe, but the depth of the sliding plane is a zone that can cause movement in the upper soil layers if the compact rock layer is disturbed. Information about the subsurface structure regarding seismic wave velocity distribution is crucial for understanding soil movement characteristics caused by earthquakes [15]. This research uses the microtremor method to map the soil condition potentially prone to movement or landslides based on the observed soil vulnerability index. The results of this study are expected to assist the local community as a reference for soil condition mapping, building planning, and geological disaster mitigation. As part of long-term planning, concrete structures should avoid weak soils or fault lines, as buildings erected in such soil conditions can have fatal consequences in natural disasters.

## 2. Material and Methods

### 2.1. Data Acquisition

The research begins with a literature review based on previous studies, data, and information on disaster events at the research site. A survey of the research site aims to conduct a preliminary study on the field conditions directly to develop a survey design. The research design is prepared on-site using the microtremor method. This is done to determine the soil vulnerability level, which will be used to map ground movements as part of geological disaster mitigation efforts, especially in that area. The research flow is illustrated in Figure 1.

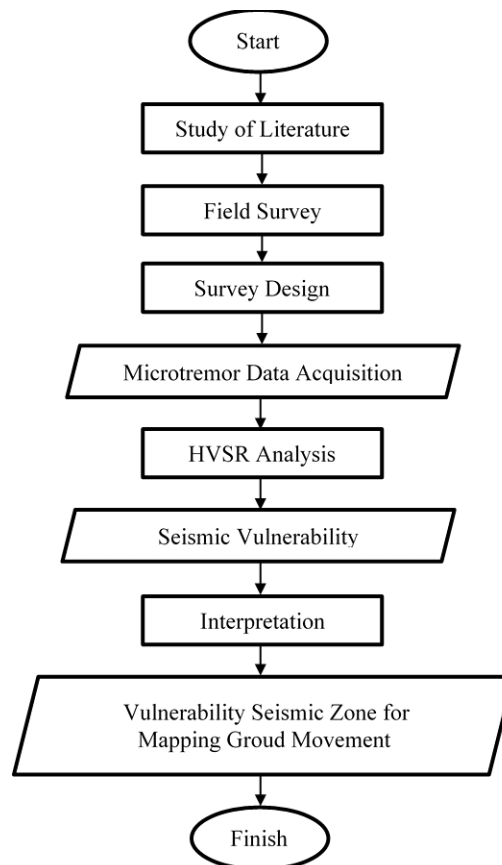


**Figure 1. Flow chart of research**

Microtremor measurements utilize several hardware components, including a DS-4A Seismometer for measuring ground vibrations at each research point, a TDL-303S Digitizer for recording ground vibrations from the seismometer, a GPS antenna connected to the digitizer for determining the position of each research point, cables for connecting the digitizer to the seismometer, a compass for determining the north direction during seismometer installation, a battery as a power source to activate the digitizer, and a laptop for analyzing the generated data (Figure 2). Additional supporting equipment includes DataPro software, Sessary Geopsy, Google Earth, Microsoft Excel, and Surfer 13.



**Figure 2. Equipment of Microtremor**

The microtremor data collection was carried out in August 2023 in Srimulyo Village, Dampit District, Malang Regency, East Java Province, Indonesia, located at coordinates  $08^{\circ}17'50.67''$  -  $08^{\circ}17'00.48''$  S and  $112^{\circ}46'37.13''$  -  $112^{\circ}46'44.49''$  E. The research site selection was based on previous studies indicating the area's potential for ground movement [4]. The microtremor measurement points were designed using a grid pattern spread across the entire research area, comprising 10 points (Figure 3), with a distance of  $\pm 100$  meters between each research point. This approach was

adopted to gain an overview of the soil vulnerability distribution at the location. The data collection process begins with determining the installation location for the seismometer, which must be positioned facing north, with the sensor placed directly on the ground surface while avoiding soft soil, mud, and bushy areas. Next, cables connect the seismometer to a TDL-303S digitizer and GPS antenna. The ground vibration recording process is carried out for a predetermined duration of  $\pm 45$  minutes with a sampling frequency of 100 Hz. During the recording process, manual notes are taken whenever there is noise from human activity, vehicles, machinery, etc. This is done to obtain signals suitable for analysis based on the SESAME European research criteria [16]. The final result of the data collection process is the recorded data of ground vibration signals in miniseed (MSD) format, which will then undergo data processing.

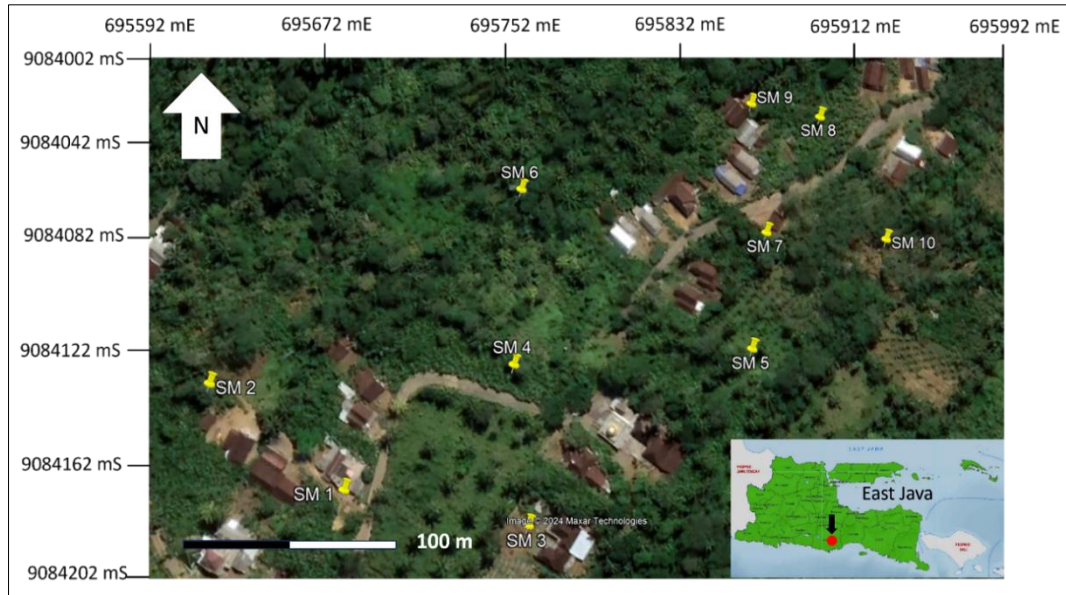


Figure 3. Microtremor Measurement Survey Design

## 2.2. Data Processing

Microtremor data processing involves using Geopsy software with data in miniseed format (MSD). The method employed is the Horizontal Vertical Spectrum Ratio (HVSr) analysis using the Fast Fourier Transform (FFT) principle. The HVSr method estimates the ratio of the Fourier spectrum of horizontal components to the vertical component [17]. In the data processing of microtremor, several steps are involved, including signal filtering using a Bandpass filter (0.5–5 Hz), which is adjusted to the low-frequency nature of microtremor signals. The signal is windowed by dividing it into several boxes (windows) to separate tremor signals from transient events. After that, a Fourier transformation is performed on each signal component to obtain the Fourier spectrum for each window. Subsequently, smoothing is applied using the Konno-Ohmachi function. The Fourier spectrum of the horizontal component is then averaged with the square root and divided by two with the spectrum of the vertical component, resulting in the average H/V spectrum. The equation representing the function in the HVSr method is shown as (Equation 1).

$$R(f) = \sqrt{\frac{H_{EW}^2(f) + H_{NS}^2(f)}{V_{UD}(f)}} \quad (1)$$

where  $R(f)$  represents the HVSr value as a function of frequency and  $H_{EW}$  and  $H_{NS}$ ; the horizontal component signals are in the East-West (E-W) and North-South (NS) directions, respectively. Meanwhile,  $V_{UD}$  is the vertical component signal in the Up-Down (U-D) direction. The result of microtremor data processing is a H/V curve that shows the dominant frequency value ( $f_0$ ) and the peak of the HVSr spectrum, which is the value of the ground spectrum amplification factor ( $A_0$ ). Based on the relation  $T = 1/f_0$ , the value of the dominant soil period ( $T_0$ ), which is used to assess the rock hardness level in the research area, can be determined. Reliable criteria for the H/V curve include three aspects indicated by (Equations 2 to 4) [16].

$$f_0 > 10/l_w \quad (2)$$

$$n_c(f_0) > 200 \quad (3)$$

$$\sigma_A(f) < 2; \text{ for } 0.5f_0 < f < 2f_0; \text{ if } f_0 > 0.5 \text{ Hz} \quad (4)$$

or:

$$\sigma_A(f) < 3; \text{ for } 0.5f_0 < f < 2f_0; \text{ if } f_0 < 0.5 \text{ Hz}$$

where the frequency  $f_0$  at the peak of H/V,  $l_w$  represents the window length,  $n_w$  is the number of selected windows on the H/V curve and  $n_c = l_w \cdot n_w \cdot f_0 \cdot \sigma_A(f)$ , the standard deviation of  $A_{H/V}(f)$ .



The analysis is conducted on various obtained parameters, including dominant frequency ( $f_0$ ), amplification factor ( $A_0$ ), and seismic vulnerability index ( $K_g$ ). The seismic vulnerability index indicates the soil layer's susceptibility to shaking, such as that caused by earthquakes. This value is derived from the square of the soil spectrum amplification value ( $A_0$ ) divided by the dominant frequency ( $f_0$ ). The results of this analysis can be used to understand the distribution of soil vulnerability values in the research area and map the conditions of soil that are potentially prone to movement or landslides. The formula for the seismic vulnerability index ( $K_g$ ) is as follows (Equation 5):

$$K_g = \frac{A_m^2}{f_0} \quad (5)$$

One factor affecting seismic vulnerability is the geomorphological condition, which relates to the soil layer's characteristics, solidity level, and sediment thickness. These factors are indicated by the soil's dominant frequency or dominant period and its spectrum amplification [18]. High seismic vulnerability index ( $K_g$ ) values are typically found in soils with soft sedimentary rock lithology, illustrating that such areas are potentially prone to earthquakes and likely to experience strong shaking. Conversely, low seismic vulnerability index ( $K_g$ ) values are generally found in soils with solid rock lithology, indicating that these areas undergo less shaking during earthquakes [19].

### 3. Result and Discussion

The HVSR analysis was conducted on ten microtremor signals recorded with three components, resulting in HVSR curves, as shown in Figure 4. The curve, the x-axis, represents the frequency values (Hz), while the y-axis represents the H/V values. The continuous black line represents the HVSR curve, and the dashed black line indicates its uncertainties. In general, the results of the HVSR curve analysis at the research location exhibit a consistent pattern: a single-peak curve. A single-peak curve indicates the presence of a thick layer of soil with significant velocity contrast in the research area. This suggests that locations SM 01, SM 02, and SM 03 have thicker soil than other locations in the research area. As for locations SM 04, SM 05, SM 06, SM 07, SM 08, SM 09, and SM 10, they show curves with wider peaks, which is assumed to be due to the presence of varying sediment structures, such as compacted sediment layers and uncompacted sediment layers. In the research area, no curves with two peaks were observed [20].

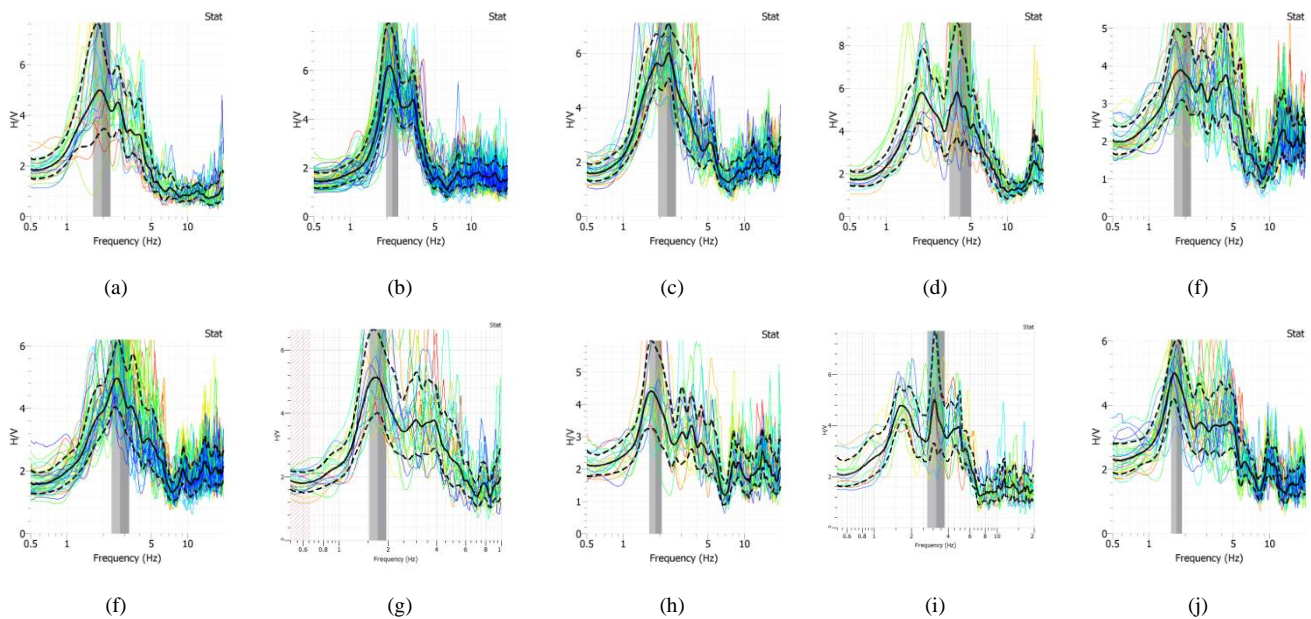


**Figure 4. HVSR Curve for the Location (a) SM 01, (b) SM 02, (c) SM 03, (d) SM 04, (e) SM 05, (f) SM 06, (g) SM 07, (h) SM 08, (i) SM 09, (j) SM 10**

#### 3.1. Dominant Parameters

HVSR analysis yields several parameters, such as the dominant frequency value ( $f_0$ ) and amplification ( $A_0$ ). The dominant frequency value ( $f_0$ ) is the maximum value of the amplitude spectrum, while the amplification value ( $A_0$ ) is the peak value of the HVSR curve, which describes the hardness or softness of the sediment or soil in the research area. Both of these parameters can be used to understand the characteristics of the subsurface layers in the studied area. The results of the HVSR analysis in the research area are shown in Table 1.

**Table 1. Results of HVSR Analysis in the Research Area**

Point	$f_0$ (Hz)	$T_0$	$A_0$	Seismic Index ( $K_g$ )
SM 01	1.943	0.515	4.949	12.606
SM 02	2.221	0.450	6.023	16.333
SM 03	2.301	0.435	5.923	15.246
SM 04	4.086	0.245	5.318	6.921
SM 05	1.897	0.527	3.860	7.854
SM 06	2.763	0.362	4.829	8.440
SM 07	1.733	0.577	5.116	15.103
SM 08	1.884	0.531	4.281	9.728
SM 09	3.202	0.312	4.792	7.172
SM 10	1.696	0.590	4.919	14.267

### 3.2. Soil Classification

Based on the dominant frequency values in Table 1, soil classification and types can be determined based on the model by Kanai (1983) [21]. This classification is crucial for understanding the local geological conditions [22]. According to the geological map of the Turen sheet [23], the lithology of the research area consists of Tertiary-aged volcanic materials, which are part of the Wuni Formation. These materials include breccia, andesite-basalt lava, tuff breccia, lahar breccia, and sandy tuff. Most of these rocks are weathered, resulting in a relatively thick layer of clay dominating the research area. The dominant frequencies obtained in the research area generally depict soft soil conditions, with the main components being alluvium and mud. The soil classification in the research location of Srimulyo Village, Dampit District, is presented in Table 2.

**Table 2. Soil Classification for Srimulyo Village, Dampit District, based on Kanai (1983)**

Point	$f_0$ (Hz)	$f_0$ range (Hz)	Class	Soil Type
SM 10	1.696			12.606
SM 07	1.733			
SM 08	1.884			
SM 05	1.897	<2.5 Hz	IV	Alluvial rock with sediment thickness >30 m
SM 01	1.943			
SM 02	2.221			
SM 03	2.301			
SM 06	2.763			
SM 09	3.202	2.5 – 4 Hz	III	Alluvial rock with a sediment thickness of 10-3- m
SM 04	4.086			

### 3.3. Distribution of Seismic Vulnerability Index ( $K_g$ )

Based on the analysis results in Tables 1 and 2, the analysis continues with interpretation to determine the distribution of dominant parameters in the research area. The distribution of dominant parameters includes maps showing the values of dominant frequency ( $f_0$ ), dominant period ( $T_0$ ), amplification ( $A_0$ ), and seismic vulnerability index ( $K_g$ ), as shown in Figure 5. The dominant frequency values ( $f_0$ ) can be classified into low and medium dominant frequencies. According to Kanai (1983), low dominant frequency values with  $f_0 < 2.5$  Hz fall into the category of alluvial soil with very thick sediment thickness (>30 m) [21]. This type is found at points SM 01, SM 02, SM 03, SM 05, SM 07, SM 08, and SM 10, with dominant frequency values ( $f_0$ ) ranging from 1.696 to 2.301 Hz. Meanwhile, medium dominant frequency values between 2.5 and 4 Hz are found at points SM 04, SM 06, and SM 09. These areas are categorized as alluvial soil with sediment thickness (>5 m) composed of gravel sand, sandy hard clay, and silt materials.

The dominant period values ( $T_0$ ) are inversely related to the dominant frequency values ( $1/f_0$ ) and are used to determine the rock hardness level in the research area. The dominant period values ( $T_0$ ) range from 0.245 to 0.590 seconds. Based on soil classification (Kanai, 1983), the research area falls into the category of soft soil with dominant period values ( $T_0$ ) ranging from 0.25 to 0.40 seconds. Meanwhile, very soft soil has dominant period values ( $T_0$ ) greater than 0.40 seconds [21].

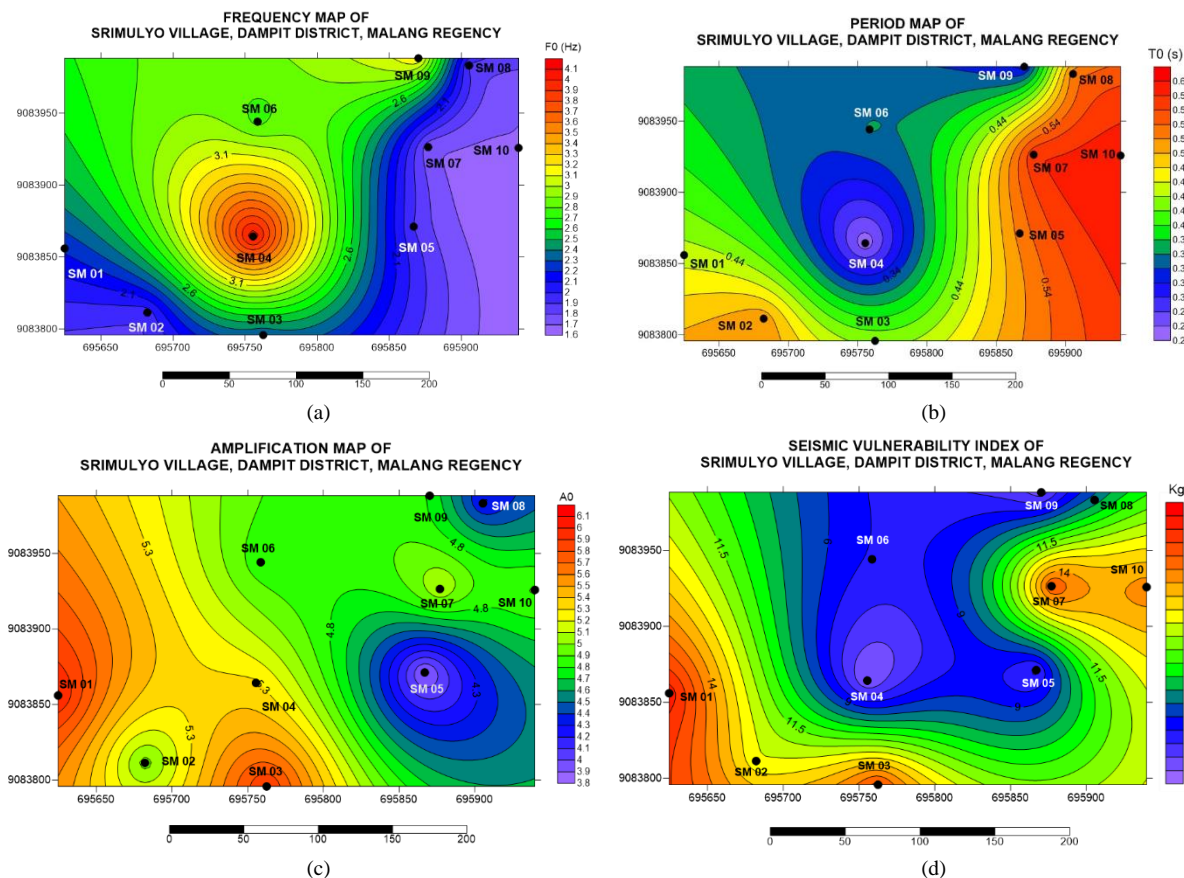


**Figure 5. Map of Dominant Parameters; (a) Dominant Frequency ( $f_0$ ), (b) Dominant Period ( $T_0$ ), (c) Amplification ( $A_0$ ), (d) Seismic Vulnerability Index ( $K_g$ )**

The amplification values ( $A_0$ ) represent the peak values of the HVSR curve, which describe the hardness or softness of the sediment or soil in the research area. In the research area, the soil amplification values range from 3.860 to 6.023. According to the Meteorology Climatology and Geophysical Agency (2010), the amplification values in the research area are classified into medium and high amplification zones [24]. The medium amplification zone is found at points SM 01, SM 03, SM 04, SM 05, SM 06, SM 07, SM 08, SM 09, and SM 10. Meanwhile, the high amplification zone is at point SM 02. According to Nakamura and Sato (2001), amplification occurs due to the seismic wave magnification caused by significant layer differences [25]. The greater the difference between layers, the larger the seismic wave amplification. In other words, the amplification value is related to sediment layers. A high amplification value indicates that the rock medium in that area is softer. Conversely, a low amplification value indicates that the rock in that area is harder.

The seismic vulnerability index ( $K_g$ ) values are used to estimate an area's vulnerability to soil movement. The research area's seismic vulnerability index values vary from 6.5 to 16.5. Low seismic vulnerability index values are distributed in the central and northern sides of the research location, ranging from 6.5 to 10. High seismic vulnerability index values are found on the research location's western, southern, and eastern sides, ranging from 10.5 to 16.5.

### 3.4. Discussion

The mapping of the seismic vulnerability index ( $K_g$ ) in the research area aims to determine the level of soil vulnerability to movements such as landslides and the effects of earthquakes in that area. Seismically vulnerable areas will have high seismic vulnerability index values. Conversely, relatively safe areas will be associated with low seismic vulnerability index values. Overlaying the seismic vulnerability index map ( $K_g$ ) on the research location results in a distribution of areas with high seismic vulnerability index values predominantly to the south of the research area (Figure 6), ranging from 10.5 to 16.5, indicated by yellow and red colors. Meanwhile, the areas around the highway are categorized as having a moderate seismic vulnerability index, with values ranging from 10 to 12.5, shown in green. Areas with low seismic vulnerability index values are scattered to the north of the research area, ranging from 6.5 to 10, represented by purple and blue colors. Consequently, it can be concluded that the highway dividing Jawar Hamlet and Srimulyo Village is a boundary between areas with high and low seismic vulnerability index values.



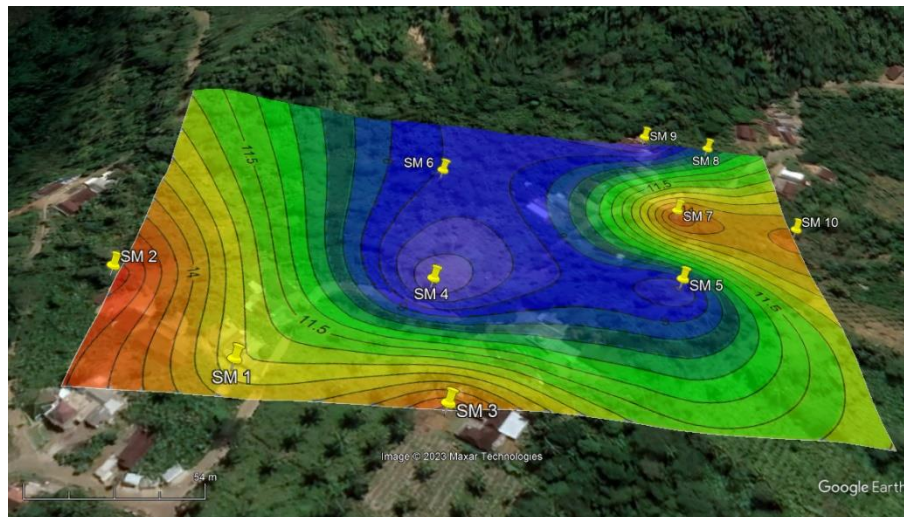


**Figure 6. Overlay of the seismic vulnerability map (Kg) on a satellite image at the research location**

Based on the seismic vulnerability index mapping in this region, the areas of concern for potential damage due to earthquakes or high soil movements are located south and southeast of the research location. Through direct observations in the research area, it is evident that the southern and southeastern parts, characterized by hills and valleys sloping towards the river to the south, have thicker sediment deposits than the north. As a result of these thick sediment deposits, the dominant frequency values to the south and southeast of Jawar Hamlet, Srimulyo Village, are lower than those in the north. Amplification values to the north of the research location are also lower than those in the southern areas. Consequently, the seismic vulnerability index values in the southern region are higher than those in the north. A similar pattern of high seismic vulnerability index values in valleys due to thick sediment deposits has been reported in the Kangra Valley region, India, resulting in high amplification during earthquake shaking [26].

Based on the seismic vulnerability index mapping in this region, the areas of concern for potential damage due to earthquakes or high soil movements are located south and southeast of the research location. Through direct observations in the research area, it is evident that the southern and southeastern parts, characterized by hills and valleys sloping towards the river to the south, have thicker sediment deposits than the north. As a result of these thick sediment deposits, the dominant frequency values to the south and southeast of Jawar Hamlet, Srimulyo Village, are lower than those in the north. Amplification values to the north of the research location are also greater than those in the southern areas. Consequently, the seismic vulnerability index values in the southern region are higher than those in the north. A similar pattern of high seismic vulnerability index values in valleys due to thick sediment deposits has been reported in the Kangra Valley region, India, resulting in high amplification during earthquake shaking [26].

The distribution of seismic vulnerability index results highlights the potential local effects of a damaging earthquake event in Jawar Hamlet, Srimulyo Village, in the future. Particular attention is drawn to buildings in the southern part, which have a high seismic vulnerability index. This is because the seismic vulnerability index allows for estimating weak points that may suffer severe damage during an earthquake [11, 27]. The seismic vulnerability index values and the level of building damage have a positive correlation of up to 80% in the case of the 2011 Van earthquake in Turkey [27]. A positive correlation between the seismic vulnerability index and earthquake damage levels is also demonstrated in the findings of Siburian et al. (2024). In their study, high seismic vulnerability index values were consistent with high ground shear strain (GSS) values in historical earthquake events in the Suban area, Curup, Rejangbong, and Bengkulu [14].

Building structure assessments in the research area also indicate that houses with structural cracks are associated with high seismic vulnerability indices, specifically 11.5, near point SM 03 (Figure 7). These houses with cracked walls are located to the south of the highway. This suggests that areas with high seismic vulnerability indices in the research area are prone to infrastructure damage due to soil movement. This is reinforced by a southeast-northwest-oriented fault to the south of the research location, which is approximately 3 kilometres to the southwest of the research site. The presence of active geological structures, such as faults, is positively correlated with seismic vulnerability in the area [28]. High seismic vulnerability index values indicate areas with thick soft sediments on the surface. This results in a significant impedance contrast between surface and subsurface rock layers. During an earthquake, seismic waves propagate from the harder subsurface medium to the softer surface medium. As a result, seismic waves are amplified [13]. If buildings on the surface are not equipped with solid construction, they will resonate. Consequently, building walls will crack and break during earthquake vibrations.



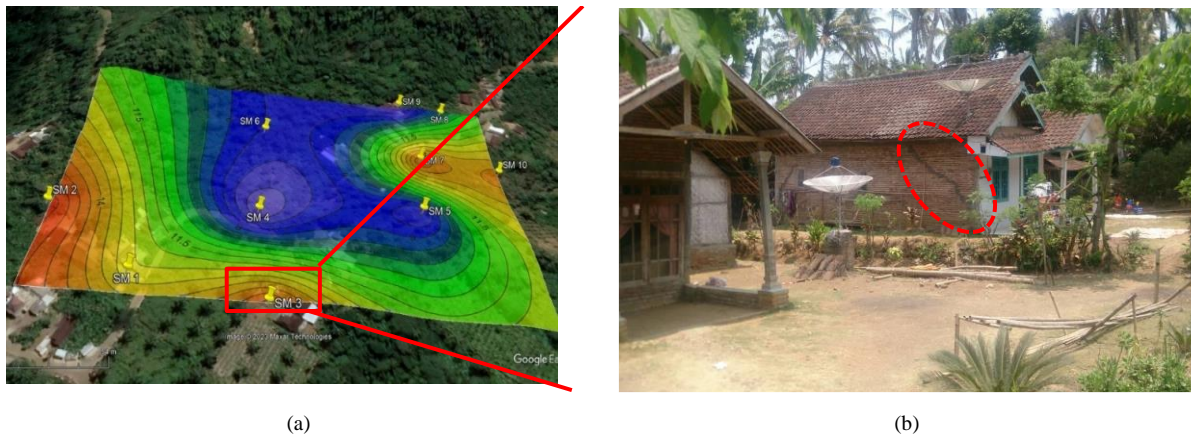


Figure 7. Map showing the locations of houses with wall cracks (5.b.) near point SM 03

In the event of an earthquake, areas with high seismic vulnerability indices are also a cause for concern because they can potentially undergo resonance, amplifying the earthquake shaking and exacerbating the resulting damage [29]. Therefore, the seismic vulnerability index mapping results in this area should be considered in infrastructure development. Therefore, this seismic vulnerability index map can serve as a reference for local government in formulating building construction standards in Srimulyo Village. High seismic vulnerability factors associated with thick sediment deposits and the presence of geological structures are considered local side effects that may lead to more severe damage than surrounding areas [30].

Previous research at this study location produced lithology information based on data obtained from drilling. Drill data near points SM 4 and SM 9 showed the presence of soft layers on the surface, consisting of silty clay at points SM 4 and SM 9, with thicknesses up to 4 meters. Based on drill data and the topography of the research site, the study also indicated the potential for creeping soil movement disasters, with the movement orientation towards the Southeast [4]. The direction of soil movement in that study aligns with the results of this research's seismic vulnerability index mapping. In the seismic vulnerability index distribution map, the vulnerable areas are spread across the Southwest, South, and Southeast of the study area. These areas are marked by high seismic vulnerability indexes, representing weak points in the research region. In previous studies, drilling points were taken at locations with low seismic vulnerability indexes. Therefore, validation through drilling at more vulnerable points, such as locations SM 1, SM 2, SM 3, or SM 7, is necessary. Based on the seismic vulnerability index mapping results, these four points are interpreted to have a thicker layer of soft sediment.

This research has provided new findings compared to previous studies in the Jawar Hamlet area, which solely relied on resistivity geoelectric surveys [4]. The current study has produced a vulnerability index map for the research location with values ranging from 10.5 to 16.5, as evidenced by houses with structural cracks. Geological structures, morphology, and sediment thickness influence the distribution of areas with high seismic vulnerability indices. To accurately determine the sediment thickness at the survey location, linear regression correlation with borehole data should be performed. Additionally, the distribution pattern of soil depth can be determined through inversion using VS30 data, representing the shear wave velocity at a depth of 30 meters at the research site. A map of seismic vulnerability indices based on depth can be created by obtaining information on soil thickness at the research location, allowing for predictions of soil movement directions at different depths.

#### 4. Conclusion

Based on the seismic vulnerability index assessment survey conducted in Jawar Hamlet, Srimulyo Village, Dampit Subdistrict, the research found a frequency range of 1.6-4.1 Hz and amplification factors ranging from 3.8 to 6.1. The seismic vulnerability index at the research location varies from 6.5 to 16.5. Areas with high seismic vulnerability indices, with  $K_g$  values greater than 11.5, are distributed to the west, south, and southeast of the research location. Field observations indicate that relatively thick sediment layers dominate the area. Due to these thick sediment deposits, the dominant frequency values to the south and southeast of Jawar Hamlet, Srimulyo Village, are lower than those in the north. Additionally, amplification values to the north of the research location are lower than those in the southern areas. As a result, the seismic vulnerability index values in the southern region are higher than those in the north. Based on mapping the seismic vulnerability index in this area, regions that need to be cautious about the potential impact of earthquakes and high soil movement activities are located to the south and southeast of the research site. This is related to the topographical factor of sloping terrain towards rivers flowing south and southeast and faults. Surveys of building conditions in the research area also indicate that houses with structural cracks are associated with high seismic vulnerability indices, specifically 11.5, near point SM 03 (Figure 7). In the event of an earthquake, areas with high seismic vulnerability indices should also be monitored because they can experience resonance, amplifying earthquake ground shaking and exacerbating the resulting damage effects.

## 5. Declarations

### 5.1. Author Contributions

Conceptualization, A.S. and S.Z.; methodology, A.S. and M.F.R.H.; software, F.H. and S.R.; validation, A.S., A.F.P., and M.A.A.; formal analysis, A.S., S.Z., F.H., S.R., and M.F.R.H.; investigation, F.R., M.F.R.H., and S.R.; resources, A.S., S.Z., and A.F.P.; data curation, A.S., M.A.A., M.F.R.H., and S.Z.; writing—original draft preparation, A.S., M.F.R.H., F.H., and S.R.; writing—review and editing, S.Z., A.F.P., and M.A.A.; visualization, F.H. and M.F.R.H.; supervision, A.S.; project administration, A.S., S.Z., and A.F.P. All authors have read and agreed to the published version of the manuscript.

### 5.2. Data Availability Statement

The data presented in this study are available on request from the corresponding author.

### 5.3. Funding and Acknowledgements

The author would like to express their gratitude to Universitas Brawijaya, Universitas Negeri Malang, and Universitas Andalas for funding this research through the Indonesian Collaborative Research Grant (RKI) Number: 10.5.59/UN32.20.1/LT/2023 from Universitas Negeri Malang, Number: 801.14/UN10.C10/TU/2023 from Brawijaya University, and Number: 5/UN16.19/PT.01.03/IS-RKI+Skema A(Mitra)/2023 from Andalas University. The author also extends their appreciation to the residents of Srimulyo Village, Dampit Subdistrict, for their support during the data collection process.

### 5.4. Conflicts of Interest

The authors declare no conflict of interest.

## 6. References

- [1] PBD Malang Regency. (2022). Data on Disaster Events in Malang Regency. Malang Regency Government: Regional Agency for Disaster Management of Malang District, Malang, Indonesia.
- [2] Imani, P., Tian, G., Hadiloo, S., & El-Raouf, A. A. (2021). Application of combined electrical resistivity tomography (ERT) and seismic refraction tomography (SRT) methods to investigate Xiaoshan District landslide site: Hangzhou, China. *Journal of Applied Geophysics*, 184, 104236. doi:10.1016/j.jappgeo.2020.104236.
- [3] Jahangiri, M., Hadianfard, M. A., & Shojaei, S. (2022). Microtremor measurements for assessing the influences of non-structural components on the modal properties and vulnerability of steel structures. *Measurement: Journal of the International Measurement Confederation*, 201, 111750. doi:10.1016/j.measurement.2022.111750.
- [4] Susilo, A., Suryo, E. A., Fitriah, F., Sutasoma, M., & Bahtiar. (2018). Preliminary study of landslide in Sri Mulyo, Malang, Indonesia using resistivity method and drilling core data. *International Journal of GEOMATE*, 15(48), 161–168. doi:10.21660/2018.48.59471.
- [5] Maha Agung, P. A., Rouf Hasan, M. F., Susilo, A., Ahmad, M. A., Bin Ahmad, M. J., Abdurrahman, U. A., Sudjianto, A. T., & Suryo, E. A. (2023). Compilation of Parameter Control for Mapping the Potential Landslide Areas. *Civil Engineering Journal*, 9(4), 974–989. doi:10.28991/CEJ-2023-09-04-016.
- [6] Rezaei, S., Shooshpasha, I., & Rezaei, H. (2020). Evaluation of landslides using ambient noise measurements (case study: Nargeschal landslide). *International Journal of Geotechnical Engineering*, 14(4), 409–419. doi:10.1080/19386362.2018.1431354.
- [7] Elbshbeshi, A., Gomaa, A., Mohamed, A., Othman, A., & Ghazala, H. (2022). Seismic hazard evaluation by employing microtremor measurements for Abu Simbel area, Aswan, Egypt. *Journal of African Earth Sciences*, 196, 104734. doi:10.1016/j.jafrearsci.2022.104734.
- [8] Liu, P. H., Wu, J. H., Lee, D. H., & Lin, Y. H. (2023). Detecting landslide vulnerability using anisotropic microtremors and vulnerability index. *Engineering Geology*, 323, 107240. doi:10.1016/j.enggeo.2023.107240.
- [9] Pornsopin, P., Pananont, P., Furlong, K. P., Chaila, S., Promsuk, C., Kamjudpai, C., & Phetkongsakul, K. (2024). Seismic Microzonation Map of Chiang Mai Basin, Thailand. *Trends in Sciences*, 21(3), 7370–7370. doi:10.48048/tis.2024.7370.
- [10] Susilo, A., Juwono, A. M., Aprilia, F., Hisyam, F., Rohmah, S., & Hasan, M. F. R. (2023). Subsurface Analysis Using Microtremor and Resistivity to Determine Soil Vulnerability and Discovery of New Local Fault. *Civil Engineering Journal*, 9(9), 2286–2299. doi:10.28991/CEJ-2023-09-09-014.
- [11] Livaoğlu, H., Irmak, T. S., & Güven, I. T. (2019). Seismic vulnerability indices of ground for Değirmendere (Kocaeli Province, Turkey). *Bulletin of Engineering Geology and the Environment*, 78(1), 507–517. doi:10.1007/s10064-017-1102-8.

- [12] Güven, İ. T. (2022). Seismic vulnerability indices for ground in Derince-Kocaeli (NW Turkey). *Environmental Earth Sciences*, 81(5), 167. doi:10.1007/s12665-022-10288-x.
- [13] Arisawadi, M., & Sastrawan, F. D. (2022). Microzonation Mapping in Supporting Construction Plan, New Capital City of Indonesia (Case Study: Sepaku Sub-district, Panajam Paser Utara Regency). 4<sup>th</sup> International Seminar on Science and Technology, 2-3 November, 2022. doi:10.2991/978-94-6463-228-6\_10.
- [14] Siburian, B. I., Marzuki, M., & Lubis, A. M. (2024). Local site effects and seismic microzonation around Suban Area, Curup Rejang Lebong, Bengkulu deduced by ambient noise measurements. *Geoenvironmental Disasters*, 11(1), 5. doi:10.1186/s40677-024-00268-7.
- [15] Chen, C. Te, Kuo, C. H., Lin, C. M., Huang, J. Y., & Wen, K. L. (2022). Investigation of shallow S-wave velocity structure and site response parameters in Taiwan by using high-density microtremor measurements. *Engineering Geology*, 297, 106498. doi:10.1016/j.enggeo.2021.106498.
- [16] European Commission. (2004). Guidelines for The Implementation of The H/V Spectral Ratio Technique on Ambient Vibrations-Measurements, Processing and Interpretations. WP12 – Deliverable D23.12. European Commission – Research General Directorate Project No. EVG1-CT-2000-00026, Brussels, Belgium.
- [17] Nakamura, Y. (1989). A method for dynamic characteristics estimation of subsurface using microtremor on the ground surface. *Railway Technical Research Institute, Quarterly Reports*, 30(1).
- [18] Rohmah, S., Susilo, A., Yudianto, D., Hisyam, F., & Suryo, E. A. (2023). Analysis of Seismic Vulnerability Index Based on Microtremor Investigation (Case Study of Majangtengah Village, Dampit, Malang Regency). 12<sup>th</sup> International Conference on Green Technology. 26-27 October, 2022, Malang, Indonesia.
- [19] Pasaribu, R. J. M., Yuliyanto, G., & Yulianto, T. (2023). Landslide Potential Analysis on New Road of Undip-Jangli Campus, Semarang Using Microtremor Method. *Cognizance Journal of Multidisciplinary Studies*, 3(6), 388–396. doi:10.47760/cognizance.2023.v03i06.025.
- [20] Noor, M. A. M., Madun, A., Kamarudin, A. F., & Daud, M. E. (2016). A Study of Geological Formation on Different Sites in Batu Pahat, Malaysia Based on HVSR Method Using Microtremor Measurement. *IOP Conference Series: Materials Science and Engineering*, 136(1), 12038. doi:10.1088/1757-899X/136/1/012038.
- [21] Kanai, K. (1983). *Engineering Seismology*. University of Tokyo Press, Tokyo, Japan.
- [22] Khalili, M., & Mirzakurdeh, A. V. (2019). Fault detection using microtremor data (HVSR-based approach) and electrical resistivity survey. *Journal of Rock Mechanics and Geotechnical Engineering*, 11(2), 400–408. doi:10.1016/j.jrmge.2018.12.003.
- [23] Sujanto, R., Hadisantono, R., Chaniago, R., & Baharuddin, R. (1992). *Geological Map of The Turen Quadrangle, Jawa*. Geological Research and Development Centre, Bandung, Indonesia.
- [24] Meteorology Climatology and Geophysical Agency. (2010). *Study of Earthquake Hazard Hazards in Bantul Regency. Special Region of Yogyakarta, Bantul, Indonesia*.
- [25] Nakamura, Y., & Sato, T. (2001). Inventory development for natural and built environments: use of seismic motion and microtremor for vulnerability assessment. 4<sup>th</sup> EQTAP Workshop in Kamakura, 3-4 December, Kamakura, Japan.
- [26] Mahajan, A. K., Kumar, P., & Kumar, P. (2021). Near-surface seismic site characterization using Nakamura-based HVSR technique in the geological complex region of Kangra Valley, northwest Himalaya, India. *Arabian Journal of Geosciences*, 14(10), 826. doi:10.1007/s12517-021-07136-w.
- [27] Akkaya, İ. (2020). Availability of seismic vulnerability index (Kg) in the assessment of building damage in Van, Eastern Turkey. *Earthquake Engineering and Engineering Vibration*, 19(1), 189–204. doi:10.1007/s11803-020-0556-z.
- [28] Banyunegoro, V. H., Muksin, U., & Idris, Y. (2020). Seismic microtremor experiment to determine seismic vulnerability of North Aceh. *IOP Conference Series: Materials Science and Engineering*, 846(1), 012053. doi:10.1088/1757-899x/846/1/012053.
- [29] Stanko, D., Markušić, S., Strelec, S., & Gazdek, M. (2017). HVSR analysis of seismic site effects and soil-structure resonance in Varaždin city (North Croatia). *Soil Dynamics and Earthquake Engineering*, 92, 666–677. doi:10.1016/j.soildyn.2016.10.022.
- [30] Akkaya, İ., Özvan, A., Tapan, M., & Şengül, M. A. (2015). Determining the site effects of 23 October 2011 earthquake (Van province, Turkey) on the rural areas using HVSR microtremor method. *Journal of Earth System Science*, 124(7), 1429–1443. doi:10.1007/s12040-015-0626-1.